

NASA  
TN  
D-4421  
=pt>2  
c.1

**NASA TECHNICAL NOTE**



**NASA TN D-4422**

NASA TN D-4422



LOAN COPY: R  
AFWL (W  
KIRTLAND AFI

# ANALYTICAL INVESTIGATION OF SUPERSONIC TURBOMACHINERY BLADING

## II - Analysis of Impulse Turbine-Blade Sections

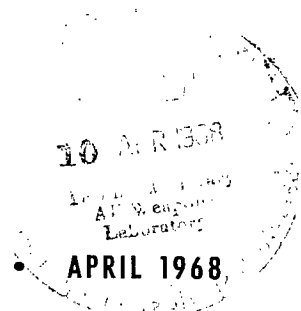
*by Louis J. Goldman*

*Lewis Research Center*

*Cleveland, Ohio*

NATIONAL AERONAUTICS AND SPACE ADMINISTRATION • WASHINGTON, D. C.

APR 1968





ANALYTICAL INVESTIGATION OF SUPERSONIC  
TURBOMACHINERY BLADING  
II - ANALYSIS OF IMPULSE TURBINE-BLADE SECTIONS

By Louis J. Goldman

Lewis Research Center  
Cleveland, Ohio

NATIONAL AERONAUTICS AND SPACE ADMINISTRATION

---

For sale by the Clearinghouse for Federal Scientific and Technical Information  
Springfield, Virginia 22151 - CFSTI price \$3.00

# ANALYTICAL INVESTIGATION OF SUPERSONIC TURBOMACHINERY BLADING

## II - ANALYSIS OF IMPULSE TURBINE-BLADE SECTIONS

by Louis J. Goldman  
Lewis Research Center

### SUMMARY

An analysis was conducted to determine the geometric characteristics of supersonic impulse turbine-blade sections. The blade sections were designed to produce vortex flow conditions within the blade passage. The effects of the lower- and upper-surface Mach numbers  $M_l$  and  $M_u$ , inlet flow angle  $\beta_i$ , and specific-heat ratio  $\gamma$  on the geometric characteristics were investigated over an inlet Mach number range of 1.5 to 5.0. Blade design limitations imposed by consideration of supersonic starting and flow separation problems as well as restriction of the axial velocity to subsonic values were also investigated over the same Mach number range.

The results of this analysis indicated that the lower-surface Mach number level  $M_l$  and the inlet flow angle  $\beta_i$  had a significant effect on blade shapes, whereas the upper-surface Mach number  $M_u$  did not. For similar surface Mach numbers the effect of specific-heat ratio  $\gamma$  on blade shape was small. Increasing  $M_l$  or decreasing  $\beta_i$  resulted in thinner blades. The blade solidities  $\sigma$  were affected significantly by all the design parameters. Increasing  $M_l$  resulted in an increase in  $\sigma$ , while increasing either  $M_u$  or  $\beta_i$  caused  $\sigma$  to decrease. For similar surface Mach numbers, increasing  $\gamma$  tends to increase  $\sigma$ . Although the design limitation considered herein places severe restrictions on the freedom on choice of the design parameters, it was still possible to obtain blades of reasonable shape and solidities that meet these restrictions.

### INTRODUCTION

In certain turbodrives power generation systems it is desired to obtain a high specific work output, with the result that large pressure ratios across the turbine are required.

This can be accomplished with either many-stage subsonic or few-stage supersonic turbines. Supersonic turbines with one or two stages are employed in special circumstances where the use of simple, low-weight systems can offset the lower efficiency expected from them because of the increased stage specific work. One such application for the supersonic turbine involves the hydrogen-fueled open-cycle auxiliary space power system described in reference 1.

To obtain the highest practical efficiency from supersonic turbines, proper design methods must be available. A method for designing supersonic blade sections is given in reference 2. The method consists of converting the uniform parallel flow at the blade inlet into a vortex flow field, turning the vortex flow, and reconvertng to a uniform parallel flow at the blade exit. The application of the design procedure involves the specification of the inlet and the outlet Mach numbers, lower- or concave-surface Mach number, upper- or convex-surface Mach number, inlet flow angle, and the specific-heat ratio of the working fluid. In general, a wide range of designs is possible by selection of these parameters. Guidance in the selection of a blade design is obtained by considering blade shape, solidity, supersonic starting, and flow separation problems. Reference 2 examines the effect of some of the design parameters for low Mach numbers and a specific-heat ratio of 1.4.

Because of the interest in hydrogen-fueled auxiliary space power systems, an analysis was conducted in order to gain a better understanding of the effects of the design parameters on the resulting blade geometry and to extend the results of reference 2 to levels of interest for such systems. A computer program was written for the design of blade sections applicable to any supersonic Mach number level and any specific-heat ratio. The mathematical description and the computer program are given in reference 3. In this report, the effects of surface Mach numbers, inlet flow angle, and specific-heat ratio on the geometric characteristics of supersonic impulse turbine-blade sections are investigated over an inlet Mach number range of 1.5 to 5.0. Blade design limitations imposed by consideration of supersonic starting and flow separation problems as well as restriction of the axial velocity to subsonic values are also investigated over the same Mach number range.

## ANALYTICAL TECHNIQUE

### Blade Description and Design

Supersonic impulse turbine-blade sections designed to produce vortex flow conditions within the blade passage (as described in ref. 2) have been used as the basis of this investigation. The blades so designed consist essentially of three major parts: (1) inlet transition arcs, (2) circular arcs, and (3) outlet transition arcs. A sketch of a typical

blade is shown in figure 1. The inlet transition arcs (lower and upper) are required to convert the assumed uniform parallel flow at the blade inlet into vortex flow. The concentric circular arcs turn and maintain the vortex flow condition. Finally, the outlet transition arcs reconvert the vortex flow into uniform parallel flow at the blade exit. Straight line segments parallel to the inlet and the outlet flow directions complete the blade.

The design of the blade sections consists principally of obtaining the required transition arcs. The method of characteristics as applied to the two-dimensional, isentropic flow of a perfect gas is utilized to calculate the transition arcs. The computer program described in reference 3 is capable of designing blade sections by this method for any Mach number level and specific-heat ratio. In general, the inlet lower transition arc reduces the Mach number from its value at the blade inlet  $M_i$  to a preselected value of lower-surface Mach number  $M_l$ , whereas the inlet upper transition arc increases the Mach number to a preselected value of upper surface Mach number  $M_u$ . The surface Mach numbers remain constant, at these preselected values, on the lower and upper circular arcs. At the outlet region the procedure is reversed. The surface Mach number variation is shown in figure 2 for a typical blade section.

The amount of flow turning produced by either the lower or the upper surface of the blade is, in general, made up of two parts (fig. 1): (1) the turning produced by the transition arc and (2) the turning produced by the circular arc. The selection of  $M_l$  and  $M_u$  (for fixed blade-inlet and -outlet Mach numbers  $M_i$  and  $M_o$ ) determines the fraction of the total flow turning produced by the transition arc for the lower and the upper surfaces, respectively. When considering flow turning at supersonic speeds, it is convenient to make use of the Prandtl-Meyer angle  $\nu$ , which is defined as the angle through which the flow must turn from a Mach number of 1 to the required Mach number. The flow turning produced by the transition arcs is then equal to differences in Prandtl-Meyer angles, being  $\nu_i - \nu_l$  and  $\nu_u - \nu_i$  for the lower and the upper inlet transition arcs, respectively. The relation between  $\nu$  and Mach number is shown in figure 3 for specific-heat ratios  $\gamma$  of 1.3, 1.4, and 1.66. As the Mach number approaches infinity,  $\nu$  approaches  $(\pi/2) \left[ \sqrt{(\gamma + 1)/(\gamma - 1)} - 1 \right]$ . For impulse blades ( $M_i = M_o$  or  $\nu_i = \nu_o$ ) if  $\nu_l = \nu_i$ , the fraction of transition turning on the lower surface is zero, and all the flow turning is accomplished by the lower circular arc. A similar situation applies to the upper surface if  $\nu_u = \nu_i$ . As  $\nu_l$  is decreased and  $\nu_u$  is increased from the value of  $\nu_i$ , the fraction of transition turning on the lower and the upper surfaces increases. For a given inlet flow angle  $\beta_i$  (for impulse blades,  $\beta_i = \beta_o$ ), the minimum value of  $\nu_l$  is  $\nu_i - \beta_i$ , and the maximum value of  $\nu_u$  is  $\nu_i + \beta_i$  (provided that  $\nu_l \geq 0$  and  $\nu_u \leq (\pi/2) \left[ \sqrt{(\gamma + 1)/(\gamma - 1)} - 1 \right]$ ), which corresponds to a fractional turning of 1 and therefore no circular arc.

## Blade Design Limitations

Establishment of supersonic flow on starting. - The mechanism by which the supersonic flow condition is established within the passage must be known if the blade sections are to be designed properly. As a first approximation it is assumed that a normal shock wave spans the blade entrance at the instant of starting (ref. 2). The permissible contraction of the blade passage is set by this condition, since the passage must be large enough to permit the shock wave to pass through. For specified surface Mach numbers (or  $\nu_l$  and  $\nu_u$ ), which fix the amount of contraction, there exists a maximum value of the inlet Mach number (or  $\nu_i$ ) for which supersonic flow can be established. The calculation procedure for the supersonic starting condition is given in reference 2. The computer program described in reference 3 is capable of making these calculations. In figures 4(a), (b), and (c) the maximum inlet Prandtl-Meyer angle  $(\nu_i)_{\max}$  for supersonic starting is plotted as a function of  $\nu_l$  and  $\nu_u$  for specific-heat ratios of 1.3, 1.4, and 1.66, respectively. The dashed line in the figures represents the case where  $\nu_u = \nu_l$ , obviously an impossible situation, but it nevertheless puts a bound on the curves. As seen from the figures, increasing  $\nu_u$  (or  $M_u$ ) at constant  $\nu_l$  or increasing  $\nu_l$  (or  $M_l$ ) at constant  $\nu_u$  increases  $(\nu_i)_{\max}$ , which is desirable from starting considerations. For similar surface Mach numbers, the maximum allowable inlet Mach number increases slightly as  $\gamma$  increases. The inlet flow angle has no theoretical effect on flow establishment.

In general, the supersonic starting condition places a severe restriction on the permissible design values of surface Mach numbers (or  $\nu_l$  and  $\nu_u$ ). This restriction can best be seen from an example. Suppose that a blade is to be designed for the following conditions: (1)  $\gamma = 1.4$ , (2)  $M_i = M_o = 2.5$  (or  $\nu_i = \nu_o = 39^\circ$ ), and (3)  $\beta_i = \beta_o = 65^\circ$ . From the previous discussion of transition turning it follows that  $(\nu_l)_{\max} = \nu_i = 39^\circ$  and  $(\nu_u)_{\min} = \nu_i = 39^\circ$ , which correspond to zero fractional transition turning. The fractional transition turning for the upper surface can be 1 if  $(\nu_u)_{\max} = \nu_i + \beta_i = 104^\circ$  (since  $(\nu_u)_{\max} < (\pi/2) \left[ \sqrt{(\gamma + 1)/(\gamma - 1)} - 1 \right]$  or  $\sim 130^\circ$ ). The fractional turning for the lower surface cannot be 1 for this example since  $\nu_l = \nu_i - \beta_i < 0$  and therefore  $(\nu_l)_{\min} = 0^\circ$ . In figure 5 the maximum inlet Prandtl-Meyer angle  $(\nu_i)_{\max}$  is plotted as a function of  $\nu_u$  for this example. For clarity only the bounds of  $\nu_l$  and  $\nu_u$  discussed previously are shown. The dashed line represents  $\nu_i = 39^\circ$ , and the region shown crosshatched would not be permissible for design purposes based on supersonic starting considerations. This restriction, unfortunately, rules out many blade designs which would otherwise be desirable. It should be emphasized that these restrictions apply only if a normal shock wave is present at the instant of starting. In some cases this restriction may not be fully applicable as indicated by the experimental investigation presented in reference 4.

Flow separation. - Consideration of the supersonic starting conditions has indicated that it is desirable to maintain the surface Mach numbers (or Prandtl-Meyer angles) at high values. Large values of  $\nu_u$ , though, would be expected to create adverse pressure gradients on the upper surface of the blade and result in flow separation. Experimental investigations of simple shapes with incompressible flow (ref. 5) have indicated that if the coefficient of pressure recovery (defined as the ratio of pressure rise to dynamic pressure) is less than about 1/2, flow separation may be avoided. This simple criterion is used herein to illustrate the design limitations due to flow separation. For supersonic velocities, the coefficient of pressure recovery at separation may be less than 1/2, and therefore the design limitations will be more restrictive than indicated. The maximum value of  $\nu_u$  that may be specified (for a given value of  $\nu_o$ ) without exceeding this criterion can be calculated as described in reference 3. Similar considerations can be applied to the lower surface, and in an analogous manner the minimum value of  $\nu_l$  (for a given value of  $\nu_i$ ) can be determined. The results of these calculations are shown in figure 6 where the maximum and minimum values of upper and lower Prandtl-Meyer angles  $(\bar{\nu}_u)_{\max}$  and  $(\bar{\nu}_l)_{\min}$  that may be specified without causing separation are plotted against  $\nu_o$  and  $\nu_i$  for specific-heat ratios of 1.3, 1.4, and 1.66. The restrictions imposed by the flow separation criterion are shown in figure 7, for the example considered previously ( $\nu_i = \nu_o = 39^\circ$ ). Figure 7 is a replot of figure 5, that is, a plot of  $(\nu_i)_{\max}$  for supersonic starting against  $\nu_u$ , on which  $(\bar{\nu}_l)_{\min}$  and  $(\bar{\nu}_u)_{\max}$  are indicated. The combined restrictions of flow separation and supersonic starting would delete the area shown cross-hatched from design considerations.

Axial velocity. - Consideration of the specification of the axial velocity or Mach number indicates two opposing tendencies. For a given Mach number, as the axial component is decreased, the nozzle angle increases, and therefore larger nozzle lengths are required. On the other hand, increasing the axial Mach number decreases the tangential velocity with a resulting decrease in turbine work. Limiting the axial Mach number to subsonic values also restricts the inlet flow angle  $\beta_i$  (for given  $M_i$ ) to values greater than  $\arccos(1/M_i)$ . For  $M_i = 2.5$ ,  $(\beta_i)_{\min} = 66.5^\circ$ , so that  $\beta_i$  would have to be specified greater than  $66.5^\circ$  if the axial velocity is to be subsonic. In some instances supersonic axial Mach numbers may be justified since under these conditions the nozzle is isolated from turbine produced disturbances. In this report both subsonic and supersonic axial Mach numbers are considered.

## RESULTS OF ANALYSIS

The results of the parametric study on turbine-blade geometric characteristics (blade shapes and solidities) are presented in this section and discussed in terms of the design limitations resulting from consideration of supersonic starting, flow sep-

aration, and supersonic axial velocity problems. The calculations were performed with the use of the computer program described in reference 3.

## Blade Shapes

The effect of the design parameters (surface Mach numbers  $M_\ell$  and  $M_u$  or surface Prandtl-Meyer angles  $\nu_\ell$  and  $\nu_u$  and inlet flow angle  $\beta_i$ ) on the turbine-blade shapes are presented in figures 8, 9, 10, and 11 for inlet Mach numbers of 1.5, 2.5, 3.5, and 5.0, respectively, and a specific-heat ratio  $\gamma$  of 1.4. The effect of  $\gamma$  on blade shapes is shown in figures 12 and 13 for specific-heat ratios of 1.3 and 1.66, respectively, and an inlet Mach number of 2.5. In each of these figures, parts (a), (b), and (c) represent the effect of  $\nu_\ell$  (or  $M_\ell$ ) on blade shape with all other parameters constant. The effect of  $\nu_u$  (or  $M_u$ ) on blade shape is obtained from part (d) by comparison with its corresponding design (same value of  $\nu_\ell$ ) given in either parts (a), (b), or (c). Finally, the effect of  $\beta_i$  (or total flow turning angle  $\theta = 2\beta_i$ ) on blade shape is shown in parts (e) and (f).

The shape of the blade is very sensitive to values of  $\nu_\ell$ , and, in general, high values of  $\nu_\ell$  result in thin blades. The effect of  $\nu_u$  on blade shape is small over the whole range of  $\nu_u$ . The flow angle  $\beta_i$  has a significant effect on blade shape, with increases in  $\beta_i$  resulting in thicker blades. For similar values of surface Mach numbers the effect of  $\gamma$  on blade shape is small.

The blade shapes shown in figures 8 to 11 have extremely thin leading and trailing edges, which would make them impractical for turbomachinery applications. Methods for creating a finite wedge angle at the leading and trailing edge are given in reference 2.

## Blade Solidity

The effect of  $\nu_\ell$  and  $\nu_u$  on turbine-blade solidity is shown in figure 14 for a total flow turning angle  $\theta$  of  $130^\circ$ . In figure 14, parts (a), (b), (c), and (d) are for inlet Mach number of 1.5, 2.5, 3.5, and 5.0, respectively, and a specific-heat ratio  $\gamma$  of 1.4. The effect of  $\gamma$  on blade solidity is shown in parts (e) and (f) for specific-heat ratios of 1.3 and 1.66, respectively, and an inlet Mach number of 2.5. The solidity  $\sigma$  is plotted as a function of  $\nu_\ell$  for representative values of  $\nu_u$  in figure 14. For each constant value of  $\nu_u$  the minimum value of  $\nu_\ell$  that will permit supersonic starting is indicated on the figure by a circle. The separation criterion is also indicated on the figure by a triangle, which represents the limits of surface Prandtl-Meyer angles that will prevent flow separation, that is,  $(\bar{\nu}_\ell)_{\min}$  and  $(\bar{\nu}_u)_{\max}$ .



Increasing  $\nu_l$  (at constant  $\nu_u$ ) tends to increase the solidity, while increasing  $\nu_u$  (at constant  $\nu_l$ ) decreases the solidity. At higher values of  $\nu_i$ , there is less change in solidity due to changes in  $\nu_u$ . For similar surface Mach numbers, increasing  $\gamma$  tends to increase the solidity.

At low values of  $\nu_u$  the supersonic starting criterion is more design restrictive than the separation criterion and, in general, blades of high solidity are required to satisfy both these limitations. As  $\nu_u$  increases, the supersonic starting criterion becomes less restrictive, while the separation criterion becomes more important. Blades designed for values of  $(\bar{\nu}_l)_{\min}$  and  $(\bar{\nu}_u)_{\max}$  will, in general, satisfy the starting criterion (except at high values of  $\nu_i$ ) and will result in the minimum blade solidity possible, since either increasing  $\nu_l$  or decreasing  $\nu_u$  will cause an increase in solidity.

The effect of total flow turning angle  $\theta$  on blade solidity is shown in figure 15 for representative blades designed so as to meet the supersonic starting and flow separation criteria. The minimum value of  $\theta$  required to limit the axial velocity to subsonic values is indicated in figure 15 by circles. Figure 15 shows that blade designs are possible that meet all three design restrictions (i. e., supersonic flow will be established on starting, the flow will not separate, and the axial velocity will be subsonic) and still have reasonable solidities (between values of 2.9 and 3.6). Of course, at the higher inlet Mach numbers large amounts of flow turning must be employed. Increasing  $\theta$  decreases the solidity.

For completeness, the pertinent design parameters, resulting blade solidities, and design limitations for the blade shapes shown in figures 8 to 13 are summarized in table I. Table I indicates that for each figure at least one blade design has been shown that meets all three design restrictions.

## SUMMARY OF RESULTS

An analysis was conducted to determine the geometric characteristics of supersonic impulse turbine-blade sections. The blade sections were designed to produce vortex flow conditions within the blade passage. The effects of the lower- and upper-surface Mach numbers  $M_l$  and  $M_u$ , inlet flow angle  $\beta_i$ , and specific-heat ratio  $\gamma$  on the geometric characteristics were investigated over an inlet Mach number range of 1.5 to 5.0. Blade design limitations imposed by consideration of supersonic starting and flow separation problems as well as restriction of the axial velocity to subsonic values were also investigated over the same Mach number range. The following results were obtained:

1. The lower-surface Mach number level  $M_l$  and the inlet flow angle  $\beta_i$  had a significant effect on blade shapes, whereas the upper-surface Mach number level  $M_u$

did not. For similar surface Mach numbers the effect of specific-heat ratio  $\gamma$  on blade shape was small. Increasing  $M_l$  or decreasing  $\beta_i$  resulted in thinner blades.

2. All the design parameters affected the blade solidities significantly. Increasing  $M_l$  resulted in an increase in solidity, while increasing either  $M_u$  or  $\beta_i$  caused the solidity to decrease. For similar surface Mach numbers, increasing  $\gamma$  tended to increase the solidity.

3. Consideration of supersonic starting, flow separation, and supersonic axial velocity problems resulted in severe blade design limitations. It is still possible, though, to design blades of reasonable shape and solidity and meet these restrictions.

Lewis Research Center,  
National Aeronautics and Space Administration,  
Cleveland, Ohio, July 25, 1967,  
128-31-02-25-22.

## REFERENCES

1. Vanco, Michael R. : Thermodynamic and Turbine Characteristics of Hydrogen-Fueled Open-Cycle Auxiliary Space Power Systems. NASA TM X-1337, 1967.
2. Boxer, Emanuel; Sterrett, James R. ; and Wlodarski, John: Application of Supersonic Vortex-Flow Theory to the Design of Supersonic Impulse Compressor - or Turbine - Blade Sections. NACA RM L52B06, 1952.
3. Goldman, Louis J. ; and Scullin, Vincent J. : Analytical Investigation of Supersonic Turbomachinery Blading. I - Computer Program for Blading Design. NASA TN D-4421, 1968.
4. Moffitt, Thomas P. : Design and Experimental Investigation of a Single-Stage Turbine with a Rotor Entering Relative Mach Number of 2. NACA RM E58F20a, 1958.
5. Schubauer, G. B. ; and Spangenberg, W. G. : Forced Mixing in Boundary Layers. Rep. no. 6107, National Bureau of Standards, Aug. 8, 1958.

TABLE I. - SUMMARY OF SUPERSONIC IMPULSE BLADE PARAMETERS

| Figure | Prandtl-Meyer angles |                        |                        | Total flow turning angle, $\theta$ | Specific-heat ratio, $\gamma$ | Solidity, $\sigma$ | Will supersonic flow be established? | Will flow separation be avoided? | Is axial velocity subsonic? |
|--------|----------------------|------------------------|------------------------|------------------------------------|-------------------------------|--------------------|--------------------------------------|----------------------------------|-----------------------------|
|        | Inlet, $\nu_i$       | Lower surface, $\nu_l$ | Upper surface, $\nu_u$ |                                    |                               |                    |                                      |                                  |                             |
| 8(a)   | 12                   | 0                      | 26                     | 130                                | 1.4                           | 2.26               | Yes                                  | Yes                              | Yes                         |
| 8(b)   | ↓                    | 4                      | 26                     | 130                                | ↓                             | 3.06               | Yes                                  | Yes                              | Yes                         |
| 8(c)   | ↓                    | 8                      | 26                     | 130                                | ↓                             | 4.02               | Yes                                  | Yes                              | Yes                         |
| 8(d)   | ↓                    | 0                      | 77                     | 130                                | ↓                             | 1.96               | Yes                                  | No                               | Yes                         |
| 8(e)   | ↓                    | 0                      | 26                     | 110                                | ↓                             | 2.96               | Yes                                  | Yes                              | Yes                         |
| 8(f)   | ↓                    | 0                      | 26                     | 150                                | ↓                             | 1.39               | Yes                                  | Yes                              | Yes                         |
| 9(a)   | 39                   | 0                      | 59                     | 130                                | ↓                             | 1.92               | No                                   | No                               | No                          |
| 9(b)   | ↓                    | 12                     | 59                     | 130                                | ↓                             | 2.56               | No                                   | No                               | No                          |
| 9(c)   | ↓                    | 18                     | 59                     | 130                                | ↓                             | 3.07               | Yes                                  | No                               | No                          |
| 9(d)   | ↓                    | 18                     | 104                    | 130                                | ↓                             | 2.95               | Yes                                  | No                               | No                          |
| 9(e)   | ↓                    | 21                     | 59                     | 120                                | ↓                             | 4.05               | Yes                                  | Yes                              | No                          |
| 9(f)   | ↓                    | 21                     | 59                     | 140                                | ↓                             | 2.76               | Yes                                  | Yes                              | Yes                         |
| 10(a)  | 59                   | 12                     | 100                    | 130                                | ↓                             | 2.30               | No                                   | No                               | No                          |
| 10(b)  | ↓                    | 34                     | 100                    | 130                                | ↓                             | 3.49               | Yes                                  | No                               | No                          |
| 10(c)  | ↓                    | 45                     | 100                    | 130                                | ↓                             | 5.56               | Yes                                  | No                               | No                          |
| 10(d)  | ↓                    | 34                     | 59                     | 130                                | ↓                             | 3.97               | No                                   | No                               | No                          |
| 10(e)  | ↓                    | 40                     | 77                     | 130                                | ↓                             | 4.48               | Yes                                  | Yes                              | No                          |
| 10(f)  | ↓                    | 40                     | 77                     | 150                                | ↓                             | 2.65               | Yes                                  | Yes                              | Yes                         |
| 11(a)  | 77                   | 39                     | 110                    | 130                                | ↓                             | 3.11               | No                                   | No                               | No                          |
| 11(b)  | ↓                    | 45                     | 110                    | 130                                | ↓                             | 3.48               | No                                   | No                               | No                          |
| 11(c)  | ↓                    | 58                     | 110                    | 130                                | ↓                             | 5.57               | Yes                                  | No                               | No                          |
| 11(d)  | ↓                    | 58                     | 77                     | 130                                | ↓                             | 6.32               | No                                   | Yes                              | No                          |
| 11(e)  | ↓                    | 62                     | 91                     | 140                                | ↓                             | 5.78               | Yes                                  | Yes                              | No                          |
| 11(f)  | ↓                    | 62                     | 91                     | 160                                | ↓                             | 2.81               | Yes                                  | Yes                              | Yes                         |
| 12(a)  | 43                   | 0                      | 68                     | 130                                | 1.3                           | 1.85               | No                                   | No                               | No                          |
| 12(b)  | ↓                    | 13                     | 68                     | 130                                | ↓                             | 2.38               | No                                   | No                               | No                          |
| 12(c)  | ↓                    | 19                     | 68                     | 130                                | ↓                             | 2.77               | Yes                                  | No                               | No                          |
| 12(d)  | ↓                    | 19                     | 108                    | 130                                | ↓                             | 2.70               | Yes                                  | No                               | No                          |
| 12(e)  | ↓                    | 25                     | 59                     | 120                                | ↓                             | 4.16               | Yes                                  | Yes                              | No                          |
| 12(f)  | ↓                    | 25                     | 59                     | 140                                | ↓                             | 2.85               | Yes                                  | Yes                              | Yes                         |
| 13(a)  | 32                   | 0                      | 45                     | 130                                | 1.66                          | 2.11               | No                                   | No                               | No                          |
| 13(b)  | ↓                    | 10                     | 45                     | 130                                | ↓                             | 3.01               | No                                   | No                               | No                          |
| 13(c)  | ↓                    | 15                     | 45                     | 130                                | ↓                             | 3.72               | Yes                                  | Yes                              | No                          |
| 13(d)  | ↓                    | 15                     | 89                     | 130                                | ↓                             | 3.47               | Yes                                  | No                               | No                          |
| 13(e)  | ↓                    | 15                     | 45                     | 120                                | ↓                             | 4.39               | Yes                                  | Yes                              | No                          |
| 13(f)  | ↓                    | 15                     | 45                     | 140                                | ↓                             | 3.00               | Yes                                  | Yes                              | Yes                         |

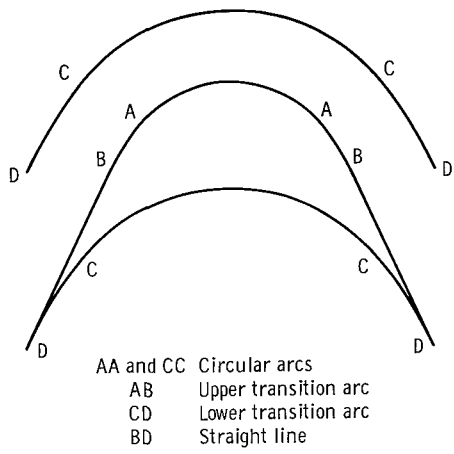


Figure 1. - Typical supersonic impulse turbine-blade section.

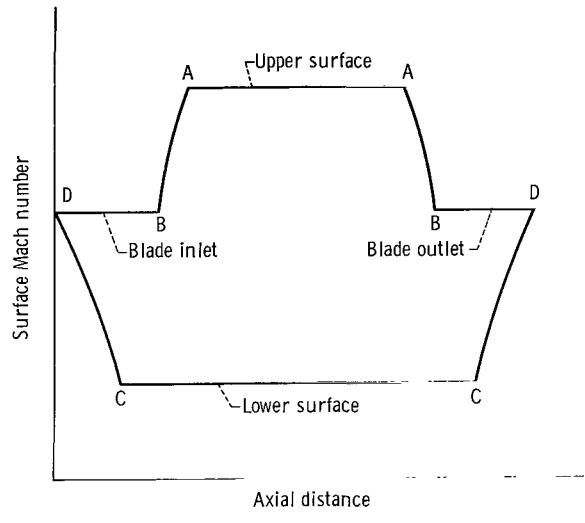


Figure 2. - Typical surface Mach number distribution for turbine-blade section.

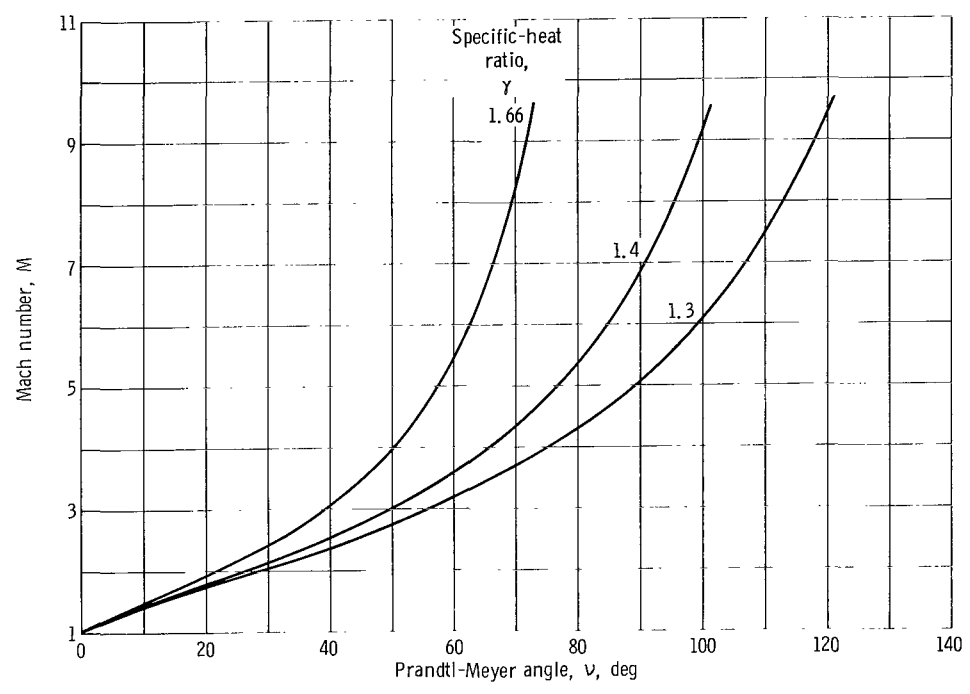
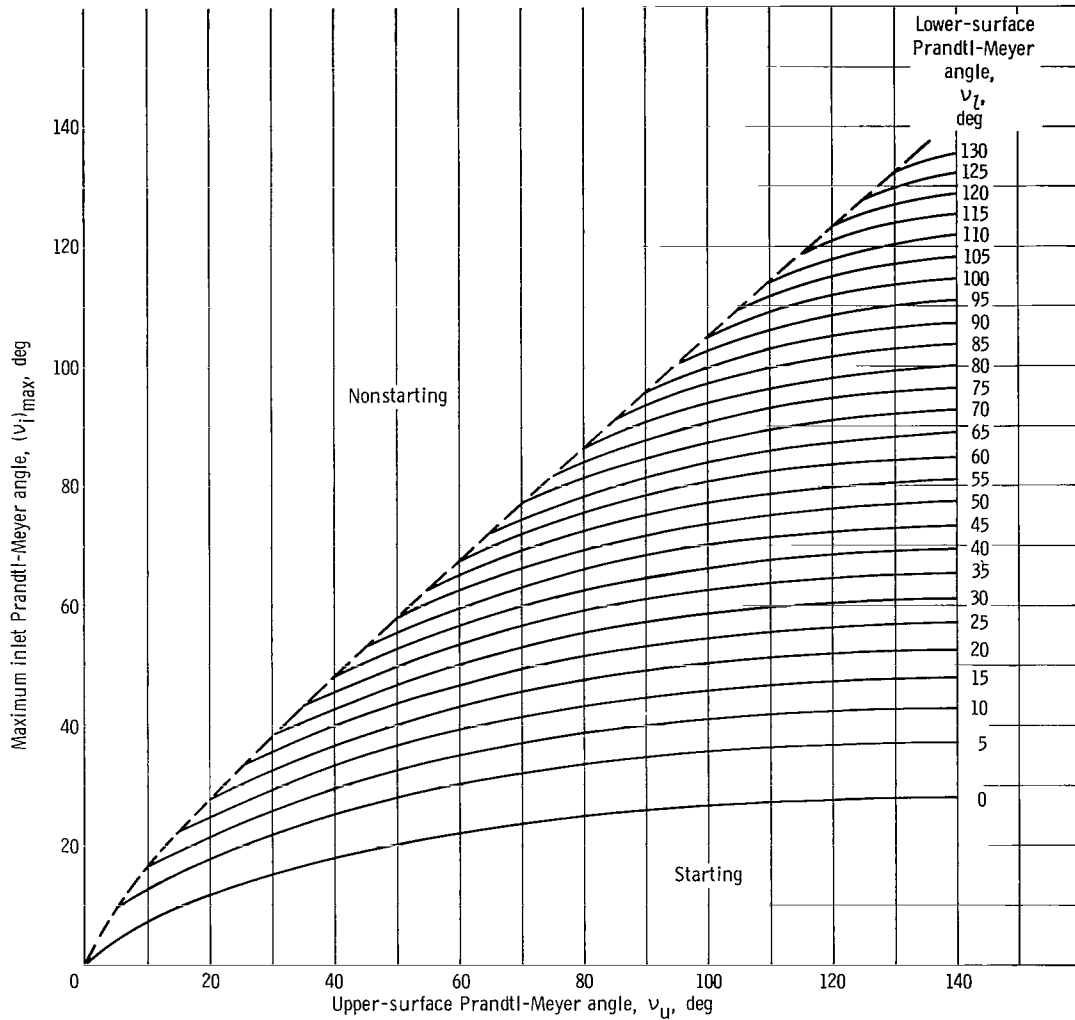
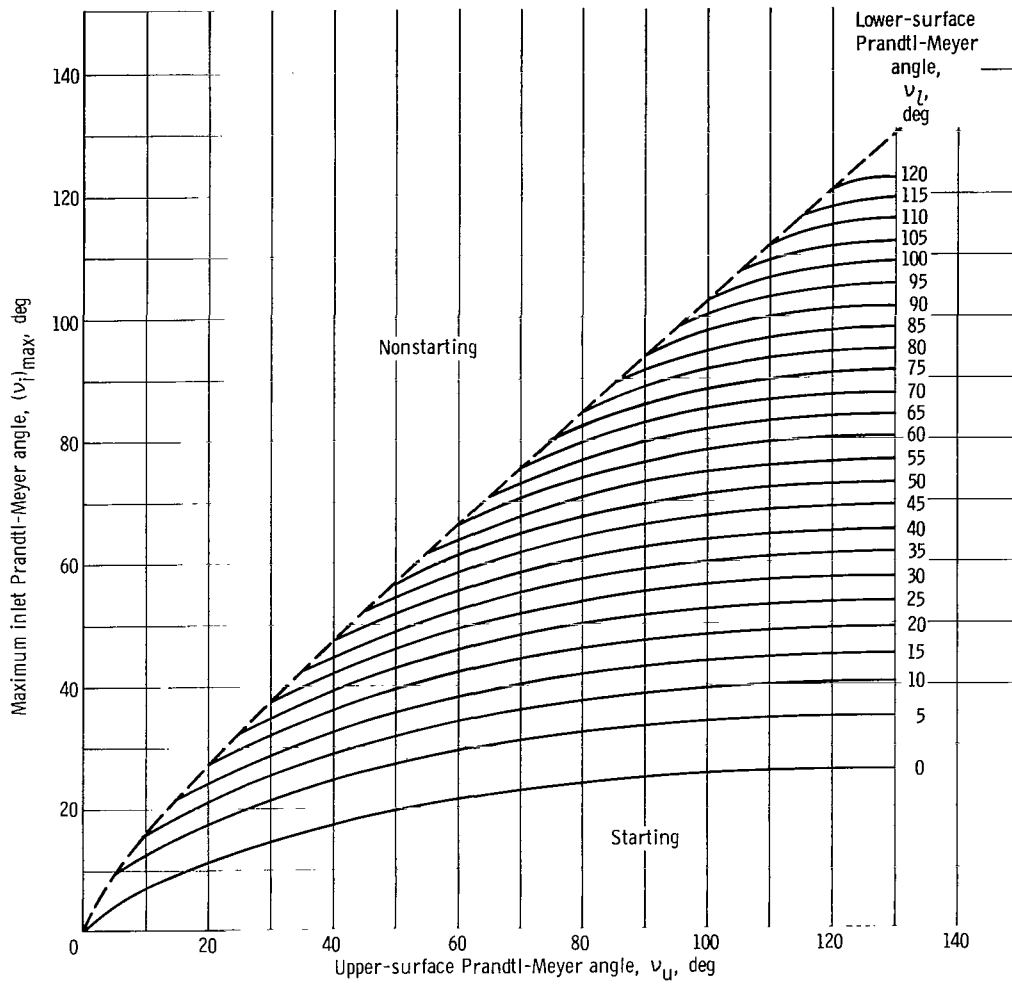


Figure 3. - Variation of Prandtl-Meyer angle with Mach number for different specific-heat ratios.



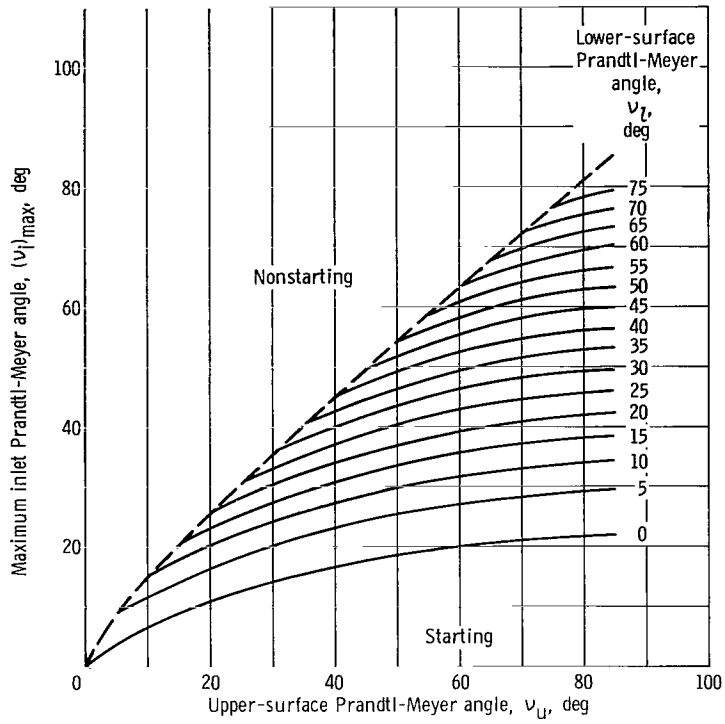
(a) Specific-heat ratio, 1.3.

Figure 4. - Maximum inlet Prandtl-Meyer angle for supersonic starting as function of surface Prandtl-Meyer angle.



(b) Specific-heat ratio, 1.4.

Figure 4. - Continued.



(c) Specific-heat ratio, 1.66.

Figure 4. - Concluded.

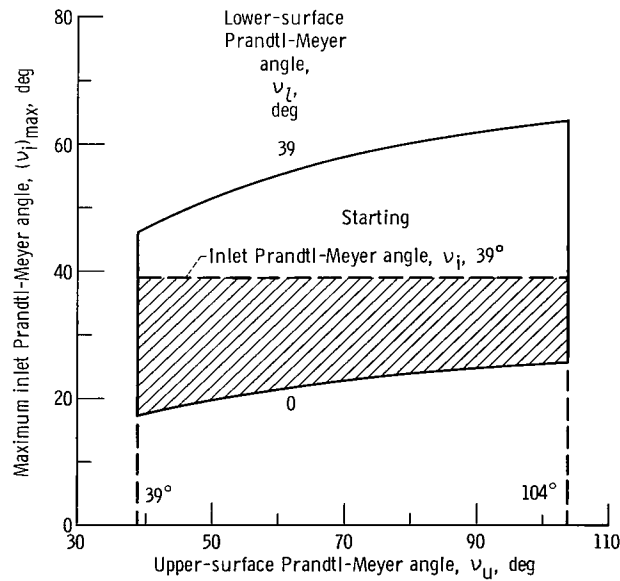


Figure 5. - Supersonic starting criterion applied to example turbine. Inlet Mach number, 2.5; inlet Prandtl-Meyer angle,  $39^\circ$ ; inlet flow angle,  $65^\circ$ .

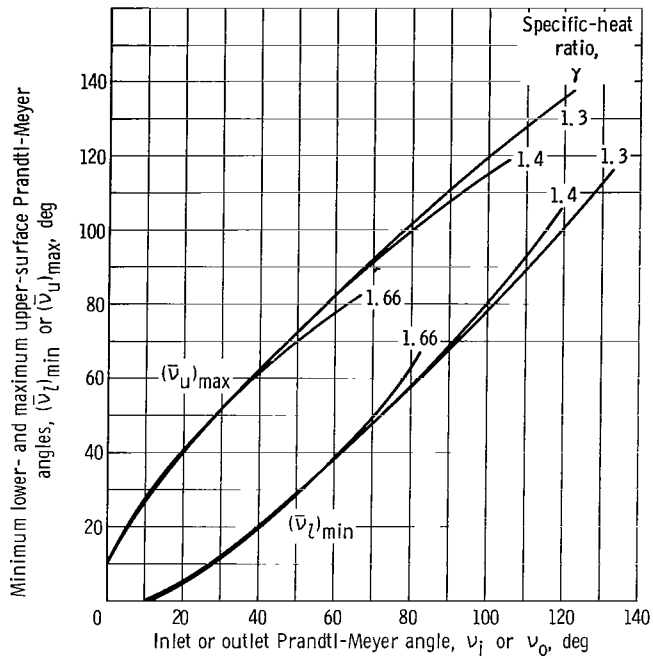


Figure 6. - Minimum lower- and maximum upper-surface Prandtl-Meyer angles to prevent flow separation as function of inlet or outlet Prandtl-Meyer angle.

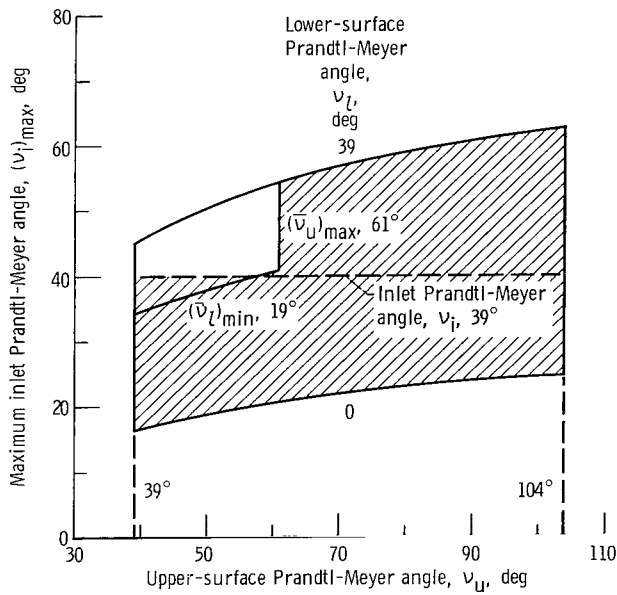
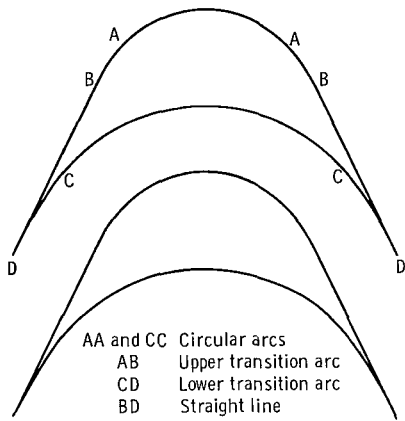
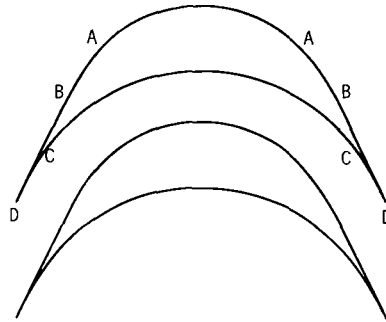


Figure 7. - Flow separation and supersonic starting criterion applied to example turbine.

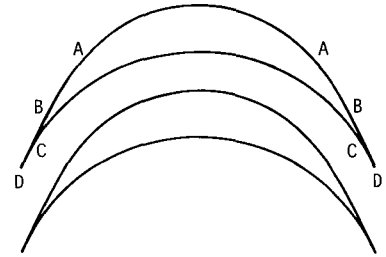




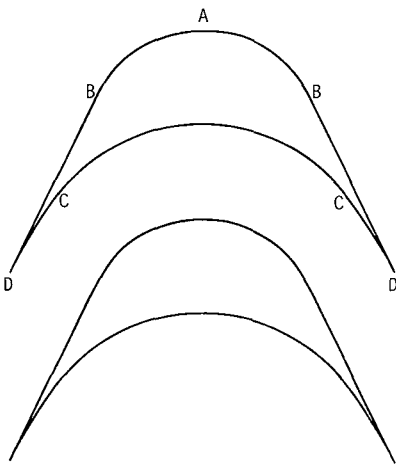
(a) Lower-surface Prandtl-Meyer angle,  $0^\circ$ ; upper-surface Prandtl-Meyer angle,  $26^\circ$ ; total flow turning angle,  $130^\circ$ ; solidity, 2.26; lower-surface Mach number, 1.0; upper-surface Mach number, 2.0.



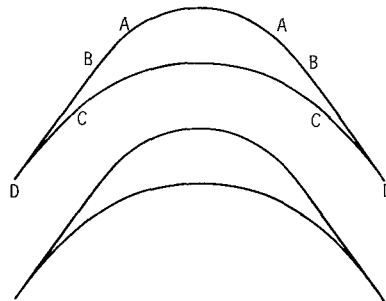
(b) Lower-surface Prandtl-Meyer angle,  $4^\circ$ ; upper-surface Prandtl-Meyer angle,  $26^\circ$ ; total flow turning angle,  $130^\circ$ ; solidity, 3.06; lower-surface Mach number, 1.2; upper-surface Mach number, 2.0.



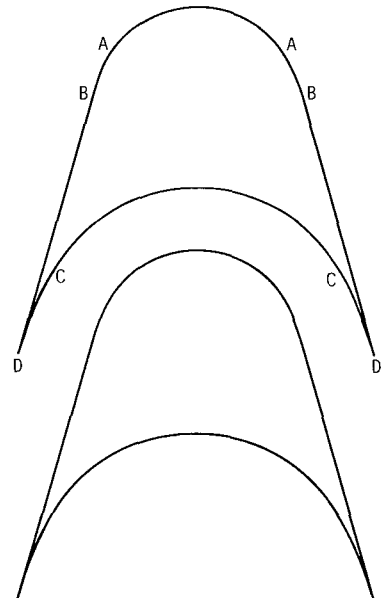
(c) Lower-surface Prandtl-Meyer angle,  $8^\circ$ ; upper-surface Prandtl-Meyer angle,  $26^\circ$ ; total flow turning angle,  $130^\circ$ ; solidity, 4.02; lower-surface Mach number, 1.4; upper-surface Mach number, 2.0.



(d) Lower-surface Prandtl-Meyer angle,  $0^\circ$ ; upper-surface Prandtl-Meyer angle,  $77^\circ$ ; total flow turning angle,  $130^\circ$ ; solidity, 1.96; lower-surface Mach number, 1.0; upper-surface Mach number, 5.0.

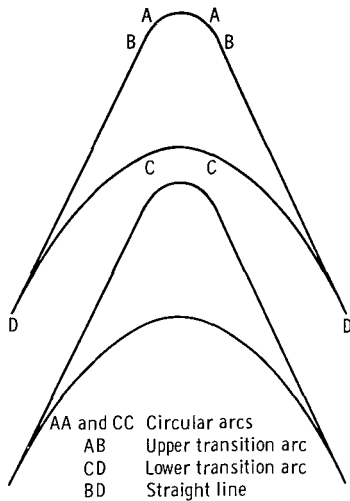


(e) Lower-surface Prandtl-Meyer angle,  $0^\circ$ ; upper-surface Prandtl-Meyer angle,  $26^\circ$ ; total flow turning angle,  $110^\circ$ ; solidity, 2.96; lower-surface Mach number, 1.0; upper-surface Mach number, 2.0.

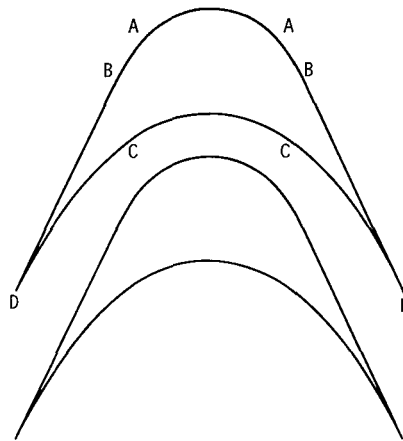


(f) Lower-surface Prandtl-Meyer angle,  $0^\circ$ ; upper-surface Prandtl-Meyer angle,  $26^\circ$ ; total flow turning angle,  $150^\circ$ ; solidity, 1.39; lower-surface Mach number, 1.0; upper-surface Mach number, 2.0.

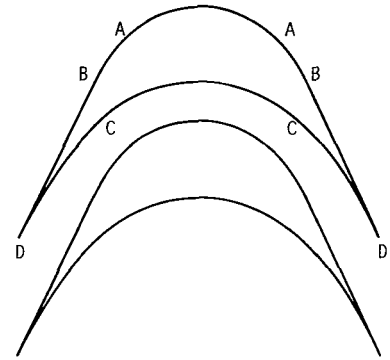
Figure 8. - Turbine-blade shapes at inlet Mach number of 1.5 (inlet Prandtl-Meyer angle,  $12^\circ$ ) and specific-heat ratio of 1.4.



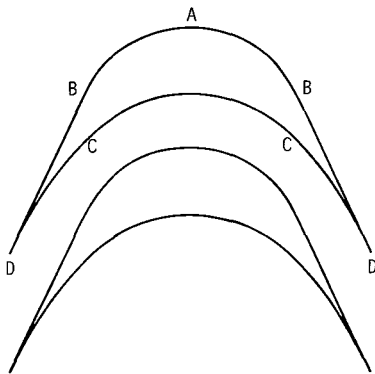
(a) Lower-surface Prandtl-Meyer angle,  $0^\circ$ ;  
 upper-surface Prandtl-Meyer angle,  $59^\circ$ ;  
 total flow turning angle,  $130^\circ$ ; solidity,  
 1.92; lower-surface Mach number, 1.0;  
 upper-surface Mach number, 3.5.



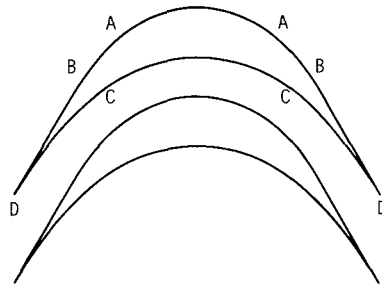
(b) Lower-surface Prandtl-Meyer angle,  $12^\circ$ ;  
 upper-surface Prandtl-Meyer angle,  $59^\circ$ ; total  
 flow turning angle,  $130^\circ$ ; solidity, 2.56; lower-  
 surface Mach number, 1.5; upper-surface Mach  
 number, 3.5.



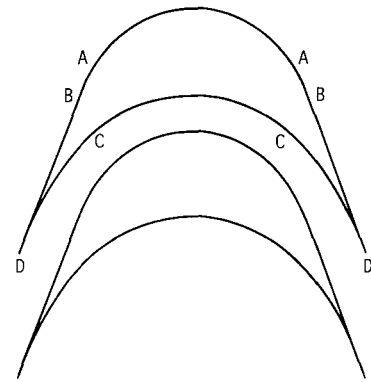
(c) Lower-surface Prandtl-Meyer angle,  $18^\circ$ ;  
 upper-surface Prandtl-Meyer angle,  $59^\circ$ ;  
 total flow turning angle,  $130^\circ$ ; solidity, 3.07;  
 lower-surface Mach number, 1.7; upper-  
 surface Mach number, 3.5.



(d) Lower-surface Prandtl-Meyer angle,  $18^\circ$ ;  
 upper-surface Prandtl-Meyer angle,  $104^\circ$ ;  
 total flow turning angle,  $130^\circ$ ; solidity, 2.95;  
 lower-surface Mach number, 1.7; upper-  
 surface Mach number, 10.7.

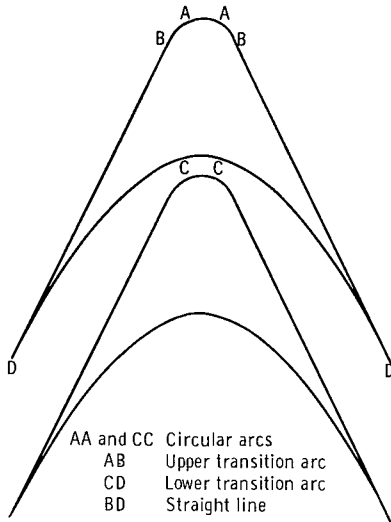


(e) Lower-surface Prandtl-Meyer angle,  $21^\circ$ ;  
 upper-surface Prandtl-Meyer angle,  $59^\circ$ ;  
 total flow turning angle,  $120^\circ$ ; solidity, 4.05;  
 lower-surface Mach number, 1.8; upper-  
 surface Mach number, 3.5.

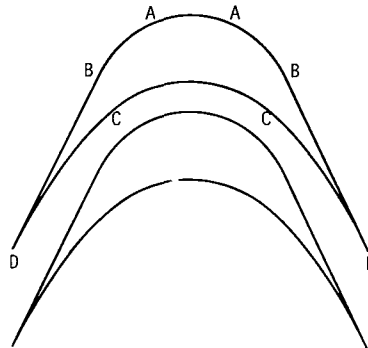


(f) Lower-surface Prandtl-Meyer angle,  $21^\circ$ ;  
 upper-surface Prandtl-Meyer angle,  $59^\circ$ ;  
 total flow turning angle,  $140^\circ$ ; solidity, 2.76;  
 lower-surface Mach number, 1.8; upper-  
 surface Mach number, 3.5.

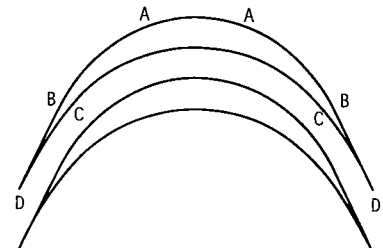
Figure 9. - Turbine-blade shapes at inlet Mach number of 2.5 (inlet Prandtl-Meyer angle,  $39^\circ$ ) and specific-heat ratio of 1.4.



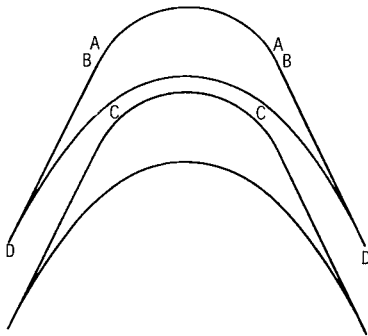
(a) Lower-surface Prandtl-Meyer angle,  $12^\circ$ ;  
 upper-surface Prandtl-Meyer angle,  $100^\circ$ ;  
 total flow turning angle,  $130^\circ$ ; solidity, 2.30;  
 lower-surface Mach number, 1.5; upper-  
 surface Mach number, 9.2.



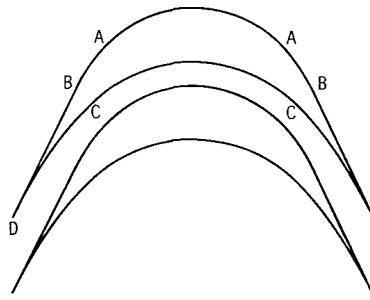
(b) Lower-surface Prandtl-Meyer angle,  $34^\circ$ ;  
 upper-surface Prandtl-Meyer angle,  $100^\circ$ ;  
 total flow turning angle,  $130^\circ$ ; solidity, 2.49;  
 lower-surface Mach number, 2.3; upper-  
 surface Mach number, 9.2.



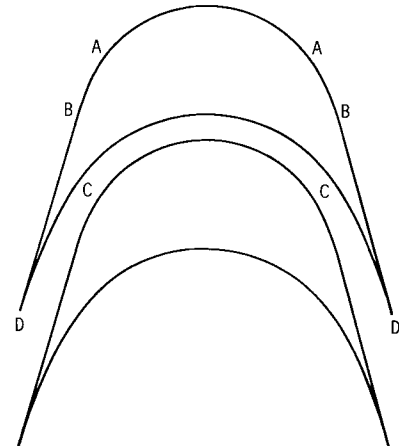
(c) Lower-surface Prandtl-Meyer angle,  $45^\circ$ ;  
 upper-surface Prandtl-Meyer angle,  $100^\circ$ ;  
 total flow turning angle,  $130^\circ$ ; solidity, 2.8;  
 lower-surface Mach number, 2.8; upper-  
 surface Mach number, 9.2.



(d) Lower-surface Prandtl-Meyer angle,  $34^\circ$ ;  
 upper-surface Prandtl-Meyer angle,  $59^\circ$ ;  
 total flow turning angle,  $130^\circ$ ; solidity, 3.97;  
 lower-surface Mach number, 2.3; upper-  
 surface Mach number, 3.5.

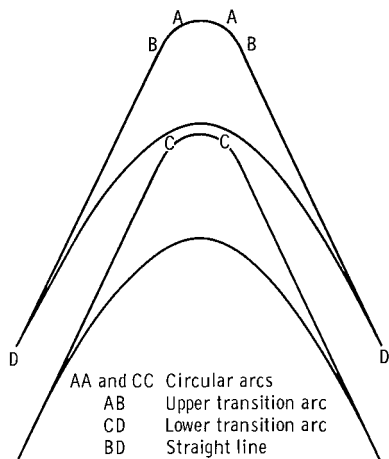


(e) Lower-surface Prandtl-Meyer angle,  $40^\circ$ ;  
 upper-surface Prandtl-Meyer angle,  $77^\circ$ ;  
 total flow turning angle,  $130^\circ$ ; solidity, 4.48;  
 lower-surface Mach number, 2.5; upper-  
 surface Mach number, 5.0.

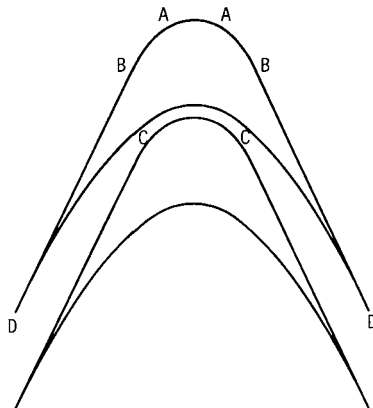


(f) Lower-surface Prandtl-Meyer angle,  $40^\circ$ ;  
 upper-surface Prandtl-Meyer angle,  $77^\circ$ ;  
 total flow turning angle,  $150^\circ$ ; solidity, 2.65;  
 lower-surface Mach number, 2.5; upper-  
 surface Mach number, 5.0.

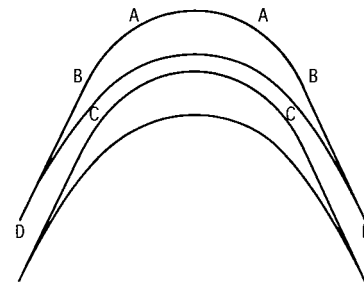
Figure 10. - Turbine-blade shapes at inlet Mach number of 3.5 (inlet Prandtl-Meyer angle,  $59^\circ$ ) and specific-heat ratio of 1.4.



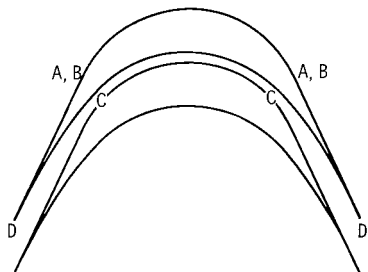
(a) Lower-surface Prandtl-Meyer angle,  $39^\circ$ ;  
 upper-surface Prandtl-Meyer angle,  $110^\circ$ ;  
 total flow turning angle,  $130^\circ$ ; solidity, 3.11;  
 lower-surface Mach number, 2.5; upper-  
 surface Mach number, 13.9.



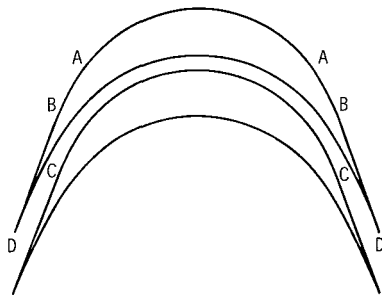
(b) Lower-surface Prandtl-Meyer angle,  $45^\circ$ ;  
 upper-surface Prandtl-Meyer angle,  $110^\circ$ ;  
 total flow turning angle,  $130^\circ$ ; solidity,  
 3.48; lower-surface Mach number, 2.8;  
 upper-surface Mach number, 13.9.



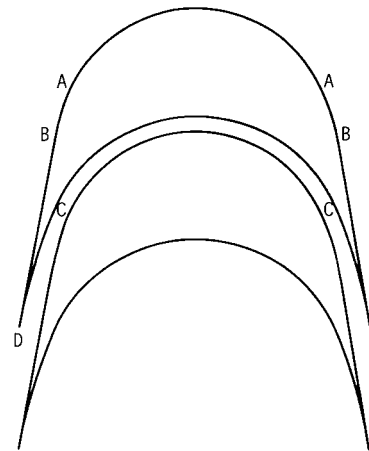
(c) Lower-surface Prandtl-Meyer angle,  $58^\circ$ ;  
 upper-surface Prandtl-Meyer angle,  $110^\circ$ ;  
 total flow turning angle,  $130^\circ$ ; solidity,  
 5.57; lower-surface Mach number, 3.5;  
 upper-surface Mach number, 13.9.



(d) Lower-surface Prandtl-Meyer angle,  $58^\circ$ ;  
 upper-surface Prandtl-Meyer angle,  $77^\circ$ ;  
 total flow turning angle,  $130^\circ$ ; solidity,  
 6.32; lower-surface Mach number, 3.5;  
 upper-surface Mach number, 5.0.

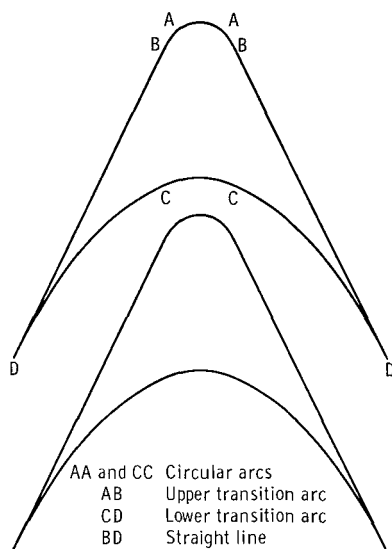


(e) Lower-surface Prandtl-Meyer angle,  $62^\circ$ ;  
 upper-surface Prandtl-Meyer angle,  $91^\circ$ ;  
 total flow turning angle,  $140^\circ$ ; solidity,  
 5.78; lower-surface Mach number, 3.7;  
 upper-surface Mach number, 7.0.

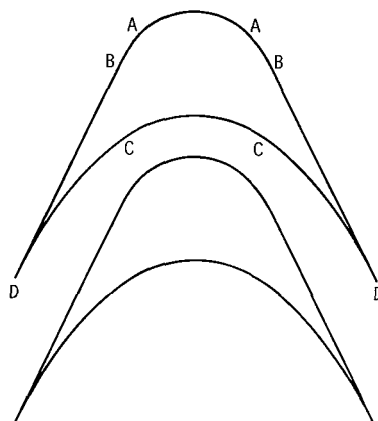


(f) Lower-surface Prandtl-Meyer angle,  $62^\circ$ ;  
 upper-surface Prandtl-Meyer angle,  $91^\circ$ ;  
 total flow turning angle,  $160^\circ$ ; solidity,  
 2.81; lower-surface Mach number, 3.7;  
 upper-surface Mach number, 7.0.

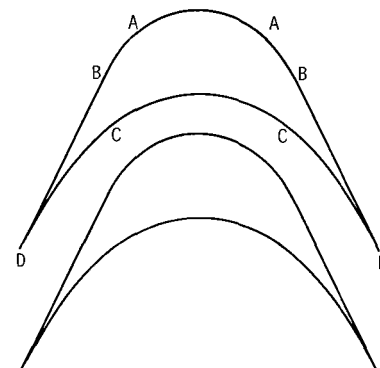
Figure 11. - Turbine-blade shapes at inlet Mach number of 5.0 (inlet Prandtl-Meyer angle,  $77^\circ$ ) and specific-heat ratio of 1.4.



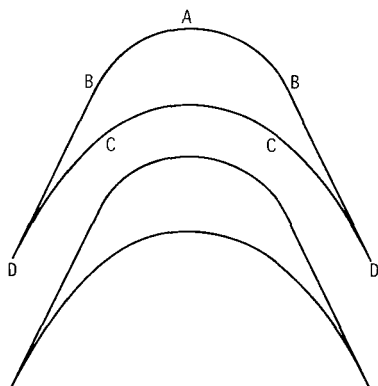
(a) Lower-surface Prandtl-Meyer angle,  $0^\circ$ ; upper-surface Prandtl-Meyer angle,  $68^\circ$ ; total flow turning angle,  $130^\circ$ ; solidity, 1.85; lower-surface Mach number, 1.0; upper-surface Mach number, 3.6.



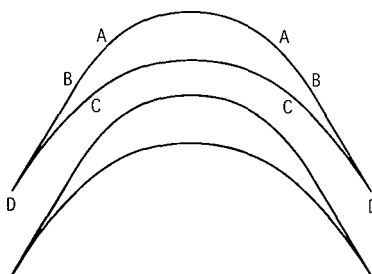
(b) Lower-surface Prandtl-Meyer angle,  $13^\circ$ ; upper-surface Prandtl-Meyer angle,  $68^\circ$ ; total flow turning angle,  $130^\circ$ ; solidity, 2.38; lower-surface Mach number, 1.5; upper-surface Mach number, 3.6.



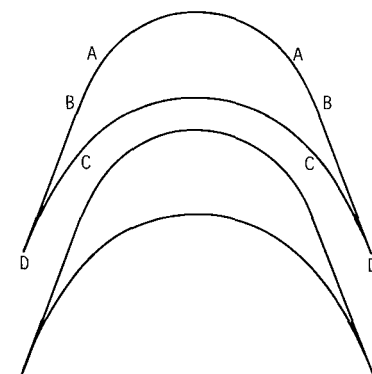
(c) Lower-surface Prandtl-Meyer angle,  $19^\circ$ ; upper-surface Prandtl-Meyer angle,  $68^\circ$ ; total flow turning angle,  $130^\circ$ ; solidity, 2.77; lower-surface Mach number, 1.7; upper-surface Mach number, 3.6.



(d) Lower-surface Prandtl-Meyer angle,  $19^\circ$ ; upper-surface Prandtl-Meyer angle,  $108^\circ$ ; total flow turning angle,  $130^\circ$ ; solidity, 2.70; lower-surface Mach number, 1.7; upper-surface Mach number, 7.1.

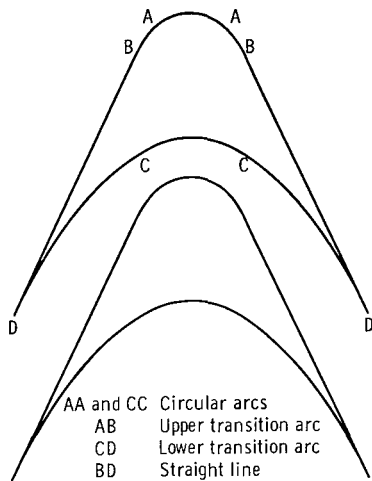


(e) Lower-surface Prandtl-Meyer angle,  $25^\circ$ ; upper-surface Prandtl-Meyer angle,  $59^\circ$ ; total flow turning angle,  $120^\circ$ ; solidity, 4.16; lower-surface Mach number, 1.9; upper-surface Mach number, 3.1.

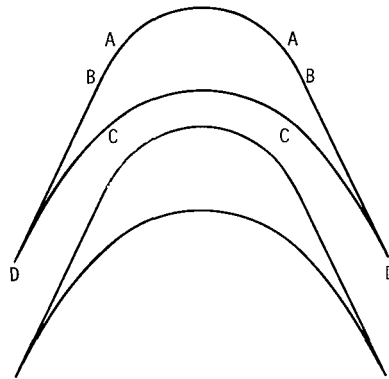


(f) Lower-surface Prandtl-Meyer angle,  $25^\circ$ ; upper-surface Prandtl-Meyer angle,  $59^\circ$ ; total flow turning angle,  $140^\circ$ ; solidity, 2.85; lower-surface Mach number, 1.9; upper-surface Mach number, 3.1.

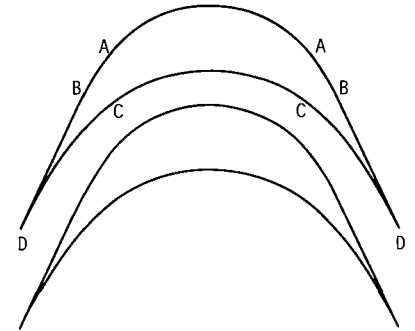
Figure 12. - Turbine-blade shapes at inlet Mach number of 2.5 (inlet Prandtl-Meyer angle,  $43^\circ$ ) and specific-heat ratio of 1.3.



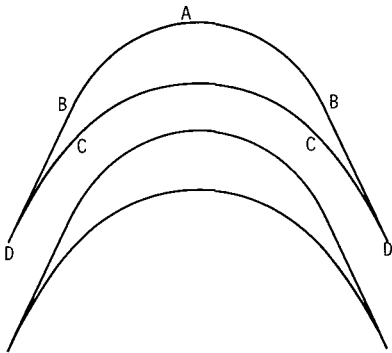
(a) Lower-surface Prandtl-Meyer angle,  $0^\circ$ ; upper-surface Prandtl-Meyer angle,  $45^\circ$ ; total flow turning angle,  $130^\circ$ ; solidity, 2.11; lower-surface Mach number, 1.0; upper-surface Mach number, 3.5.



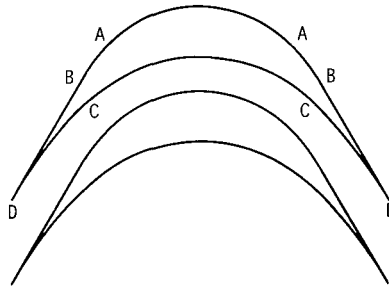
(b) Lower-surface Prandtl-Meyer angle,  $10^\circ$ ; upper-surface Prandtl-Meyer angle,  $45^\circ$ ; total flow turning angle,  $130^\circ$ ; solidity, 3.01; lower-surface Mach number, 1.5; upper-surface Mach number, 3.5.



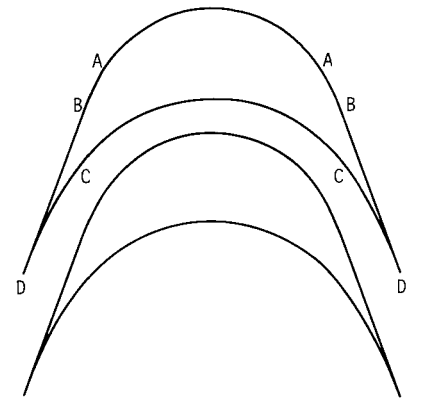
(c) Lower-surface Prandtl-Meyer angle,  $15^\circ$ ; upper-surface Prandtl-Meyer angle,  $45^\circ$ ; total flow turning angle,  $130^\circ$ ; solidity, 3.72; lower-surface Mach number, 1.7; upper-surface Mach number, 3.5.



(d) Lower-surface Prandtl-Meyer angle,  $15^\circ$ ; upper-surface Prandtl-Meyer angle,  $89^\circ$ ; total flow turning angle,  $130^\circ$ ; solidity, 3.47; lower-surface Mach number, 1.7; upper-surface Mach number, 103.



(e) Lower-surface Prandtl-Meyer angle,  $15^\circ$ ; upper-surface Prandtl-Meyer angle,  $45^\circ$ ; total flow turning angle,  $120^\circ$ ; solidity, 4.39; lower-surface Mach number, 1.7; upper-surface Mach number, 3.5.



(f) Lower-surface Prandtl-Meyer angle,  $15^\circ$ ; upper-surface Prandtl-Meyer angle,  $45^\circ$ ; total flow turning angle,  $140^\circ$ ; solidity, 3.00; lower-surface Mach number, 1.7; upper-surface Mach number, 3.5.

Figure 13. - Turbine-blade shapes at inlet Mach number of 2.5 (inlet Prandtl-Meyer angle,  $32^\circ$ ) and specific-heat ratio of 1.66.

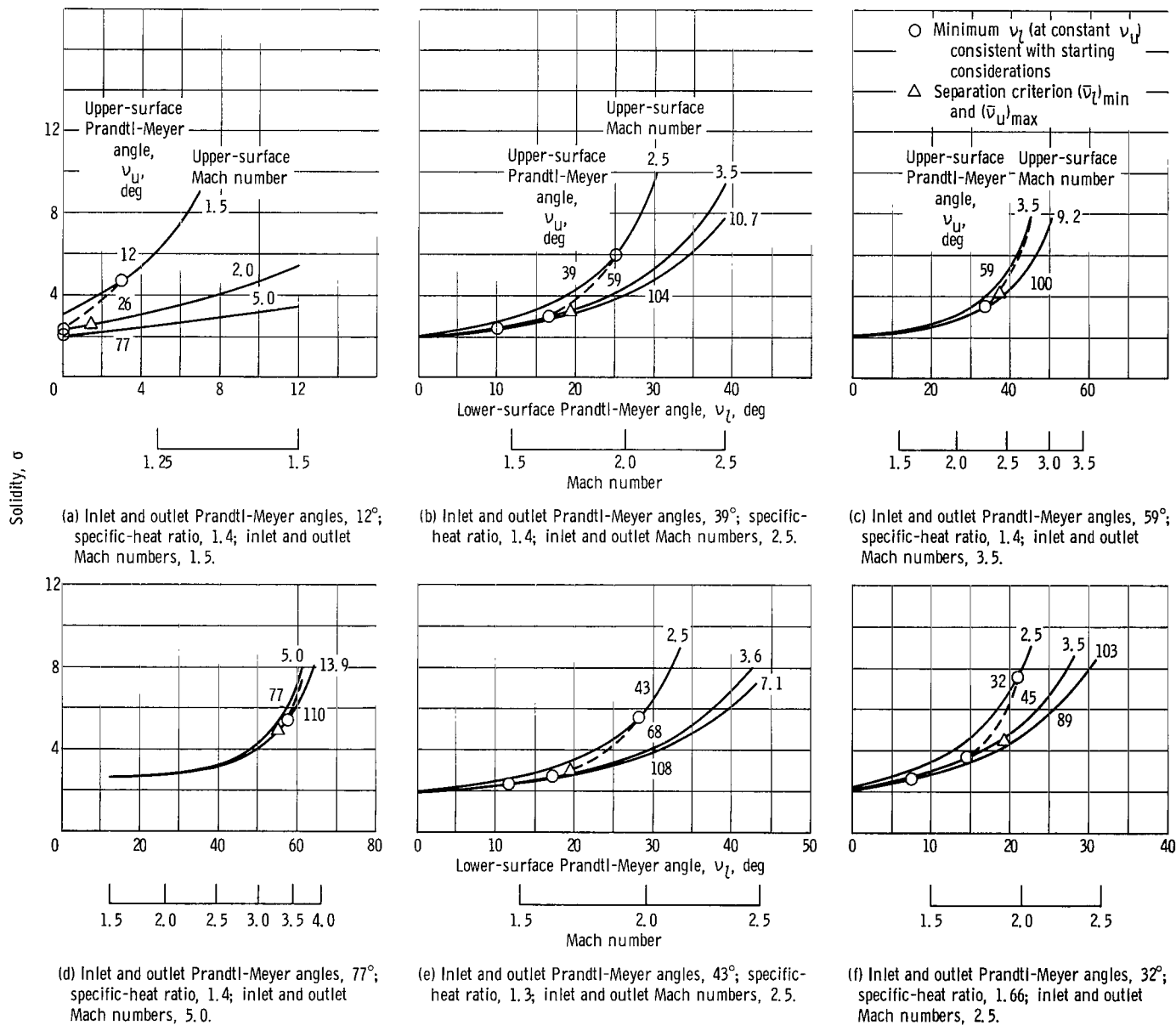


Figure 14. - Solidity characteristics of turbine blades. Total flow turning angle,  $130^\circ$ .

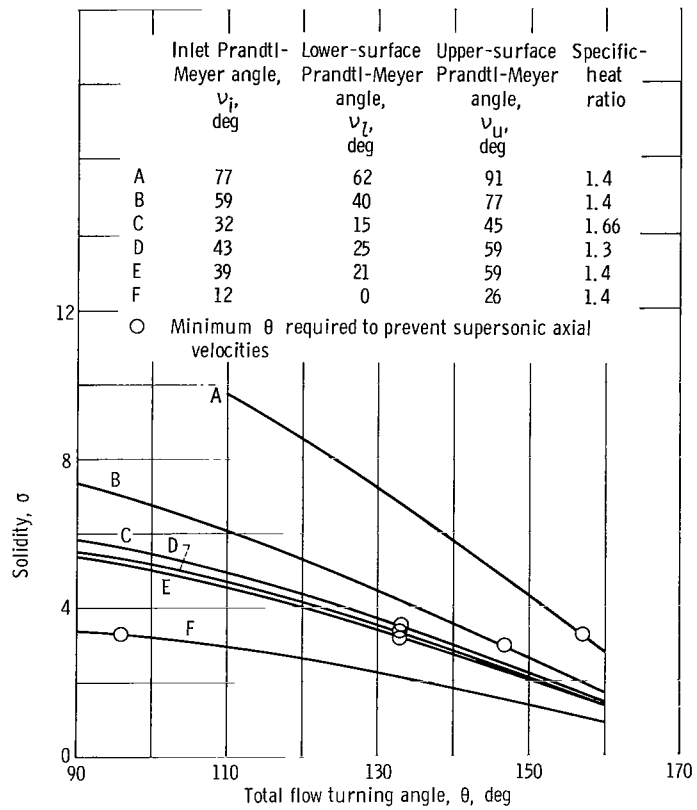


Figure 15. - Effect of total flow turning angle on solidity.



050 001 26 51 305 68092 00903  
AIR FORCE WEAPONS LABORATORY/AFWL/  
WRIGHT AIR FORCE BASE, NEW MEXICO 87117

AIR MAIL PERMIT NO. 70 CANADA, FIRST CLASS

POSTMASTER: If Undeliverable (Section 158  
Postal Manual) Do Not Return

*"The aeronautical and space activities of the United States shall be conducted so as to contribute . . . to the expansion of human knowledge of phenomena in the atmosphere and space. The Administration shall provide for the widest practicable and appropriate dissemination of information concerning its activities and the results thereof."*

—NATIONAL AERONAUTICS AND SPACE ACT OF 1958

## NASA SCIENTIFIC AND TECHNICAL PUBLICATIONS

**TECHNICAL REPORTS:** Scientific and technical information considered important, complete, and a lasting contribution to existing knowledge.

**TECHNICAL NOTES:** Information less broad in scope but nevertheless of importance as a contribution to existing knowledge.

**TECHNICAL MEMORANDUMS:** Information receiving limited distribution because of preliminary data, security classification, or other reasons.

**CONTRACTOR REPORTS:** Scientific and technical information generated under a NASA contract or grant and considered an important contribution to existing knowledge.

**TECHNICAL TRANSLATIONS:** Information published in a foreign language considered to merit NASA distribution in English.

**SPECIAL PUBLICATIONS:** Information derived from or of value to NASA activities. Publications include conference proceedings, monographs, data compilations, handbooks, sourcebooks, and special bibliographies.

**TECHNOLOGY UTILIZATION PUBLICATIONS:** Information on technology used by NASA that may be of particular interest in commercial and other non-aerospace applications. Publications include Tech Briefs, Technology Utilization Reports and Notes, and Technology Surveys.

*Details on the availability of these publications may be obtained from:*

SCIENTIFIC AND TECHNICAL INFORMATION DIVISION  
NATIONAL AERONAUTICS AND SPACE ADMINISTRATION

Washington, D.C. 20546